

SIMULATION OF THE ELECTROSTATIC CHARGING OF PHILAE ON 67P/CHURYUMOV-GERASIMENKO AND OF ITS INTERACTION WITH THE DUSTS.

S. L. G. Hess¹, P. Sarrailh¹, J.-C. Mat eo-V el ez¹, J. Forest², B. Jeanty-Ruard² and F. Cipriani³

Abstract. ROSETTA’s probe Philae landed on a dust covered soil. This dust may be ejected from the ground through many mechanisms (other than spacecraft landing) : micro-meteorite impacts, electrostatic charging and soil outgassing. In any cases, the dust grains charge electrostatically in the ambient plasma and this charge impacts the dust interaction with the spacecraft, which is itself differentially charged due to its partial exposure to the solar UV light. Using the DUST addition to the Spacecraft-Plasma Interaction Software (SPIS) routinely used to compute the charge state of the spacecraft surfaces, we simulate the electrostatic charging of Philae as well as its dust environment. SPIS-DUST allows one to compute the electrostatic charging of the dust grains on the ground and in the plasma, and to model their ejection and their recollection by the probe. We simulated one cometary day of the Philae environment at different distances from the sun to observe the variation of the dust collection with Philae’s local time.

Keywords: Comet, Rosetta, Philae, Dust

1 Introduction

The Rosetta spacecraft reached comet 67P/Churyumov-Gerasimenko on August 2014 and was inserted into orbit, on November Philae separated from Rosetta and landed on the comet. After a first touchdown close to the expected landing site, Philae bounced and finally stopped in a more chaotic region after several touchdowns (Biele et al. 2015). In particular, the lander attitude and its position close to a cliff jeopardized its chances to survive. Eventually, the probe received enough power from the sun later in Rosetta’s mission and brought new information on the comet surface. Among Philae missions, the Dust Impact Monitor collects dusts. Although it is expected that most of the dusts will be ejected from the ground because of the sublimation of volatile materials in the soil, these neutral dust grains will interact with the plasma and acquire an electric charge that can modify their interaction with Philae and its instruments. The present study concentrates on the determination of the importance of dust charging on the dust collection by Philae.

2 Numerical Model

2.1 SPIS

The Spacecraft-Plasma Interaction Software (SPIS) is an open source tool (available along with a more detailed description at <http://dev.spis.org>) for the simulation of the charging of materials in a plasma environment (Roussel et al. 2008, 2012). First developed to simulate the charge of artificial satellites in space (Roussel et al. 2008), it was later developed to simulate plasma experiments on the ground (Mat eo-V el ez et al. 2008), scientific probes aboard interplanetary probes (Guillemant et al. 2012, 2013), and is currently being extended to allow for the simulation of the dust charging and transport (Hess et al. 2015). This simulation scheme is essentially electrostatic, even though a background magnetic field can be set that acts on the particle motions. The electric

¹ ONERA - The French Aerospace Lab, 31055 Toulouse, France

² Artnum, 75010 Paris, France

³ ESA/ESTEC, 2201 AZ Noordwijk, The Netherlands

potential is computed by solving the Poisson equation across the simulation domain.

SPIS allows for the use of multiple schemes for the description of the particle populations such as Particle-In-Cell (PIC) and Poisson-Boltzman, multiple spatial scales (unstructured tetrahedral meshes), and multiple times scales for the simulation of the plasma and the interactions with materials (Roussel et al. 2012).

In the present simulation, we model the bulk solar wind species (electrons and protons) as PIC populations. A minor (100 m^{-3}) hot (1 keV) component of each solar wind species is added to model the plasma environment in the comet wake. This hot component is not drifting and is modeled by a Poisson-Boltzmann approximation. Neutrals and dust grains are modeled as PIC populations. All populations have the same time step than the Poisson equation solver, except the dust grains that have a time step 10^5 times larger. This permits us to numerically speed-up the dust motion and to allow for their simulation in realistic times, but it has no impact on the physical model since the dust characteristic time scales remain larger than that of the other species.



Fig. 1. Geometry of the simulation domain. The domain cross-section is 50x50 meter. Philae is close to the center. The comet rotation axis is approximately directed toward the top of the page on this picture.

In a similar way, the spacecraft and comet surface potentials are computed over a larger time step than the plasma potential. This permits us to compute these potentials in realistic times without modifying the results of the simulation since we are only interested by long scale variations and not by transient phenomena that could occur at the plasma time scales.

The simulation domain is based on the digital terrain model published by the CNES, but was reproduced by hand to simply the topology. The domain cross-section is 50x50 meters and the box height is 130 m. This height is needed to correctly reproduce the potential barrier above the sunlit surfaces. Philae is at its real size, but its geometry was simplified, as its legs and instruments are not reproduced. The mesh size is fixed but adapted to the expected Debye length across the simulation domain. The typical cell size is 8 m on the open boundary and 1 m on the surface.

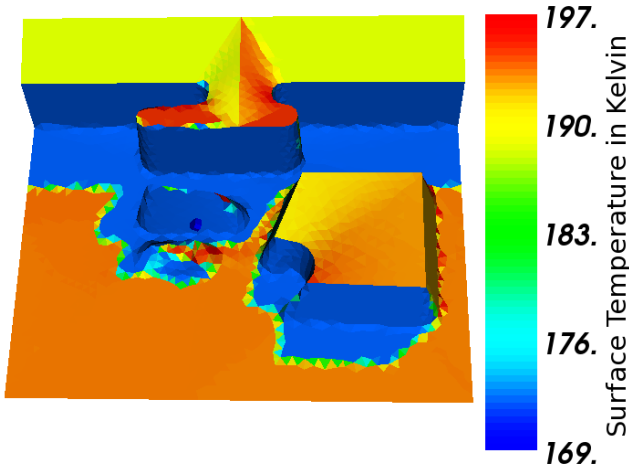


Fig. 2. Temperature of the comet surface computed using the simple model implemented in SPIS. The local time is noon. Philae surface temperatures are not computed.

Parameter	Value
cold e^- , H^+ densities	$2E6 \text{ m}^{-3}$
hot e^- , H^+ densities	100 m^{-3}
cold e^- , H^+ bulk velocities	400 km.s^{-1}
cold e^- , H^+ temperature	10 eV
hot e^- , H^+ temperature	1 keV
albedo A	0.04
solar flux Φ_{\odot}	340 W.m^{-2}
emissivity ϵ	1
soil thermal inertia [†] \mathcal{I}	$450 \text{ W.m}^{-2}.\text{K}^{-1}.\text{s}^{1/2}$
ice fraction f_{H_2O}	0.3
ice specific heat \mathcal{L}	1100 J/K/kg
isotherm temperature [†] T_0	184 K

Table 1. Parameters used in the plasma and thermal models. [†]Parameters that are computed from material characteristics and from the model.

2.2 Dust physics

The dust particles and their physics have been introduced in a new version of SPIS that will be publicly released in 2015, as the SPIS 5.2 version. The dust population differs from the plasma or neutral population in that all

particles do not share the same characteristics (different radii,...) that may evolve with time (charge). SPIS allows the user to define distributions for the characteristics of the dust on the ground, in particular for their radii. SPIS computes the dust interaction with the plasma (plasma collection and secondary emission) and with the solar photons (photo-emission) to determine the charge state of the dust grains in the plasma.

The charge evolution both influences and depends on the dust motion in the plasma. It also participate to the dust ejection from the ground. The computation of the dust charging on the ground is more complex than that in the plasma, as a dusty surface is a complex composite material for which no physical models exist that describe its electrostatic behavior. SPIS computes the dust grain charging on the ground by assimilating the irregular surface to a "bed of nails" of different sizes on which the charge and the electric field are computed using a tip effect model. The size distribution of the tips and the charge and electric field enhancements are related through the model, which is described in details in Hess et al. (2015). If the electrostatic forces are strong enough and cannot be balanced by gravitational and cohesive forces, the dust is ejected.

In the present simulation we use the material characteristics of the lunar regolith to model the comet soil (see description in Hess et al. 2015). It is now set that 67P soil is composed of carbon-rich regolith (Capaccioni et al. 2015) which strongly differs from lunar silicates, but in absence of a complete characterization of this material, we use a better know material instead.

2.3 Thermal model and sublimation

The dust ejection from the ground due to electrostatic charging may not be the dominant process on a comet, where the sublimation of the volatile material (water and carbon oxides ices) in the ground may carry small dusts. In the present study, we developed a model of dust ejection caused by volatile material sublimation. In this case, the dust grain ejection occurs because of the neutral pressure rather than because of the electrostatic force. Thus, dust ejection strongly depends on the neutral outgassing flux, which itself depends on the soil composition and on its thermal behavior. Several studies have been - and are still- performed to give accurate models of the comet thermal behavior, taking into account many physical processes. Such a model is however out of the scope of the present study. We rather introduced a very simple toy-model of the surface temperature of the comet, T , which only depends on the instantaneous lighting of the surface:

$$\epsilon\sigma T^4 - (1 - A)\mathcal{T}\Phi_{\odot} + \mathcal{I}(T - T_0)\sqrt{4/P} + f_{H_2O}\rho_{sat}v_T\mathcal{L} = 0 \quad (2.1)$$

First term stands for the power radiated by the ground, depending on the emissivity, ϵ . Second term stands for the incoming power from the sun, which depends on the albedo, A and on a transfer function \mathcal{T} . Third term stands for the power diffused in depth, depending of the thermal inertia, \mathcal{I} , on the comet period, P , and on an isotherm temperature, T_0 taken as the average temperature of the comet. Last term stand for the power lost by sublimation, depending on the water ice fraction, f_{H_2O} , the saturation density, ρ_{sat} , the vapor atoms thermal velocity across the surface, v_T , and the specific heat, \mathcal{L} . Parameters that have been used are shown in Table 1. Because we assumed lunar regolith in an ice matrice, neglecting porosity, our estimate of the thermal inertia is several times larger than that deduced from observations (Gulkis et al. 2015; Spohn et al. 2015), but is in the range of older models Davidsson & Gutiérrez (2005). At 2 AU, the surface temperature varies between 169 K and 198 K, whereas more complex simulation, like that of Tennishev et al. (2011), give value between 165 K and 197 K. We consider than this small discrepancy is not of primary importance given the actual knowledge of the comet surface and the accuracy needed for the present study.

3 Simulations

We perform simulations of Philae and comet soil charging in a solar wind condition at 2 AU from the sun: the UV flux is 0.25 times that at Earth, the solar wind density is 2.10^6 m^{-3} , and all the other parameters are the same than for the lunar case. The simulations are first run in a 12:00LT configuration for the equivalent of 1.13 hours in order to initialize it and then for 12.5 hours with the direction of the solar wind species bulk velocities and of the photon changing in accordance with the local time.

In order to investigate the role of dust charging in the interaction between Philae and its environment, we perform three simulations: first one only takes into account the dust ejection due to its charging on the ground, the outgassing and the neutral dust ejection by outgassing are turned off. In a second simulation, we take into account the dust ejection due to outgassing along with the electrostatic charging. In a last simulation, we turn off the electrostatic charging of the dusts, both on the ground and in the plasma, i.e. all dust grains are neutral.

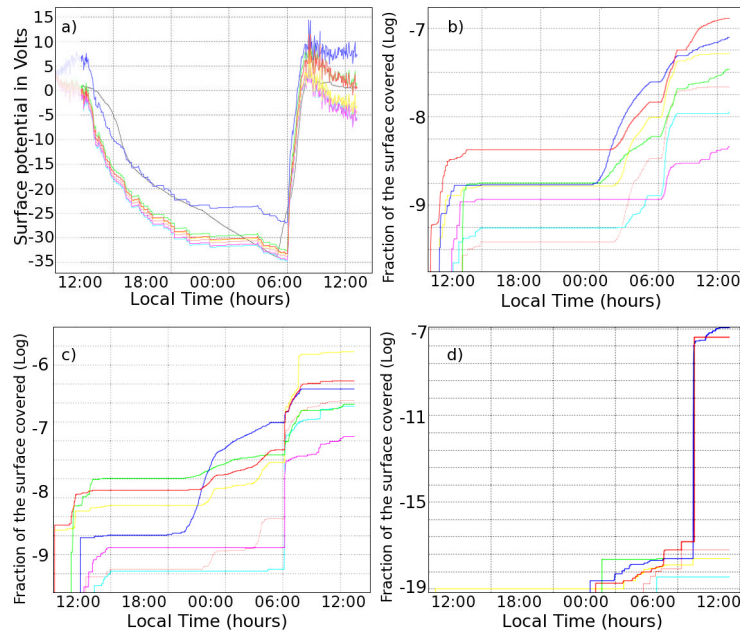


Fig. 3. Evolution of the surface potentials on the different electrical nodes (a). Fraction of the surface covered for runs with electrostatic charging and no outgassing (b), outgassing and charging (c) outgassing and no charging (d). Color code: black= comet surface, dark blue= Philae top, light blue= Philae bottom and instrument side. Red, yellow, green, pink, purple= Philae solar panel sides, counted in the clockwise direction (when seen from above) starting after the instrument side (In this configuration, red is directed upward and purple downward).

Panel a of Fig. 3 shows the evolution of the averaged surface potential over different elements: the comet surface (black), Philae's top solar panel (dark blue) and the other surface elements of Philae (see Figure caption for details). At noon, all of the surfaces are a few Volts positive, because of the photo-electron emission. Shortly after 13:00LT the surface potentials drop abruptly as Philae gets into the shade. The surface potential only decrease noticeably after 15:00LT. The surface potentials of Philae decrease until 00:00LT when they stabilize thanks to the secondary emission caused by the hot plasma populations. The ground secondary emission yield is much lower than that of Philae surfaces, so its potential continues to decrease. Then, all potentials increase abruptly around 06:00LT when the surfaces are sunlit again.

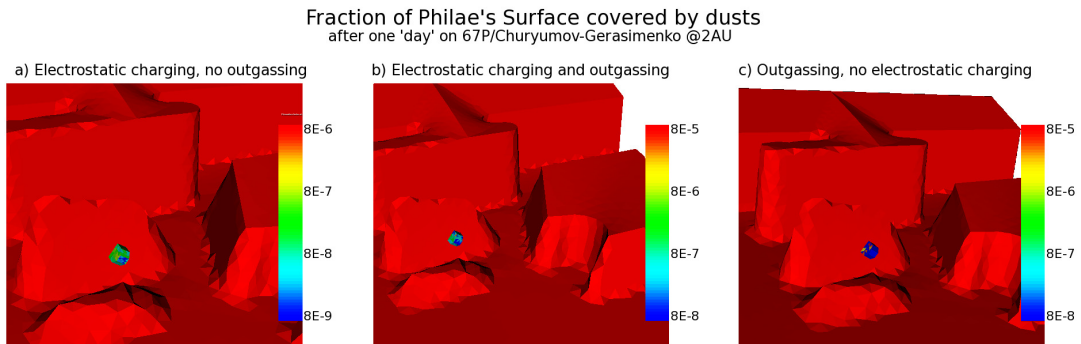


Fig. 4. Fraction of the Philae's surface covered by dust, in log scale, after a simulation lasting for one cometary day ($\simeq 12\text{h}30$). **Left:** In the case for which the dusts are allowed to charge electrostatically in the plasma and on the surface, leading to their ejection. The dust ejection due to outgassing is not included in this simulation. **Middle:** In the case for which the dust ejection due to outgassing is simulated and the dusts are allowed to charge electrostatically in the plasma and on the surface, leading to their ejection. **Right:** In the case for which the dust ejection due to outgassing is simulated but the dusts are not allowed to charge electrostatically neither the plasma nor on the surface.

The other panels of 3 show the evolution of the fraction of the surface cover by dusts (same color code, but the ground is not plotted), for the three cases we simulated. In the case without electrostatic charging, the dust deposit is very low and only concerns the panel facing the $+z$ direction. The two other cases are very similar, except for a dust deposit about one order of magnitude larger in the case with outgassing. The differences in the amount of dust deposited can be clearly seen on Fig. 4 which shows maps on the fraction of the surface covered by dust in the three cases we simulated.

For simulations with electrostatic charging, the dust collection by the surfaces is directly related to the exposure to the sunlight: the top solar panel (dark blue) of Philae is amongst the most covered, whereas the solar panel of Philae which is directed toward the ground (purple) is the less covered. It is also highly correlated with the potential difference between the surfaces and the ground. The time evolution clearly shows that dust grains are collected once a surface is more positive than the ground. This is due to the fact that the ground potential is negative, so that the emitted dusts are negatively charged and attracted by positive potentials. Most of the dust is collected around 06:00LT, when the sunrise.

4 Conclusions

We performed simple simulation of Philae on 67P/Churyumov Gerasimenko using generic parameters for the comet composition that would have to be refined using the results of the ongoing experiments to accurately model the environment of Philae. Nonetheless, our purpose was to investigate the effect of the electrostatic charging of the dust grains on their interaction with Philae. We showed that even if the dominant dust production mechanism is the ejection of neutral dust caused by the sublimation of volatile material in the soil, the subsequent charging of the dust increased the dust collection by about an order of magnitude. This is an important effect that should be taken into account to interpret Philae's dust measurements.

The SPIS-DUST development has been funded under ESA Contract No. 4000107327/12/NL/AK

References

- Biele, J., Ulamec, S., Maibaum, M., et al. 2015, *Science*, 349, 019816
- Capaccioni, F., Coradini, A., Filacchione, G., et al. 2015, *Science*, 347
- Davidsson, B. J. R. & Gutiérrez, P. J. 2005, *Icarus*, 176, 453
- Guillemant, S., Génot, V., Matéo-Vélez, J.-C., Ergun, R., & Louarn, P. 2012, *Ann. Geophys.*, 30, 1075
- Guillemant, S., Génot, V., Vélez, J.-C., et al. 2013, *IEEE Transactions on Plasma Science*, 41, 3338
- Gulkis, S., Allen, M., von Allmen, P., et al. 2015, *Science*, 347
- Hess, S., Sarrailh, P., Matéo-Vélez, J.-C., et al. 2015, *IEEE Transactions on Plasma Science*, 43, 2799
- Matéo-Vélez, J.-C., Roussel, J., Sarrail, D., et al. 2008, *IEEE Transactions on Plasma Science*, 36, 2369
- Roussel, J., Dufour, G., Matéo-Vélez, J.-C., et al. 2012, *IEEE Transactions on Plasma Science*, 40, 183
- Roussel, J., Rogier, F., Dufour, G., et al. 2008, *IEEE Transactions on Plasma Science*, 36, 2360
- Spohn, T., Knollenberg, J., Ball, A. J., et al. 2015, *Science*, 349, 020464
- Tenishev, V., Combi, M. R., & Rubin, M. 2011, *The Astrophysical Journal*, 732, 104